



HAL
open science

Impact of Spacing and Orientation on the Scar Threshold With a High-Density Grid Catheter

Masateru Takigawa, Jatin Relan, Takeshi Kitamura, Claire A. Martin, Steven Kim, Ruairidh Martin, Ghassen Cheniti, Konstantinos Vlachos, Grégoire Massoulié, Antonio Frontera, et al.

► **To cite this version:**

Masateru Takigawa, Jatin Relan, Takeshi Kitamura, Claire A. Martin, Steven Kim, et al.. Impact of Spacing and Orientation on the Scar Threshold With a High-Density Grid Catheter. *Circulation. Arrhythmia and electrophysiology*, 2019, 12 (9), 10.1161/CIRCEP.119.007158 . hal-03033103

HAL Id: hal-03033103

<https://hal.science/hal-03033103>

Submitted on 26 Oct 2021

HAL is a multi-disciplinary open access archive for the deposit and dissemination of scientific research documents, whether they are published or not. The documents may come from teaching and research institutions in France or abroad, or from public or private research centers.

L'archive ouverte pluridisciplinaire **HAL**, est destinée au dépôt et à la diffusion de documents scientifiques de niveau recherche, publiés ou non, émanant des établissements d'enseignement et de recherche français ou étrangers, des laboratoires publics ou privés.

ORIGINAL ARTICLE

Impact of Spacing and Orientation on the Scar Threshold With a High-Density Grid Catheter

BACKGROUND: Multipolar catheters are increasingly used for high-density mapping. However, the threshold to define scar areas has not been well described for each configuration. We sought to elucidate the impact of bipolar spacing and orientation on the optimal threshold to match magnetic resonance imaging-defined scar.

METHOD: The HD-Grid catheter uniquely allows for different spatially stable bipolar configurations to be tested. We analyzed the electrograms with settings of HD-16 (3 mm spacing in both along and across bipoles) and HD-32 (1 mm spacing in along bipoles and 3 mm spacing in across bipoles) and determined the optimal cutoff for scar detection in 6 infarcted sheep.

RESULTS: From 456 total acquisition sites (mean 76 ± 12 per case), 14 750 points with the HD-16 and 32 286 points with the HD-32 configuration for bipolar electrograms were analyzed. For bipolar voltages, the optimal cutoff value to detect the magnetic resonance imaging-defined scar based on the Youden's Index, and the area under the receiver operating characteristic curve (AUROC) differed depending on the spacing and orientation of bipoles; across 0.84 mV (AUROC, 0.920; 95% CI, 0.911–0.928), along 0.76 mV (AUROC, 0.903; 95% CI, 0.893–0.912), north-east direction 0.95 mV (AUROC, 0.923; 95% CI, 0.913–0.932), and south-east direction, 0.87 mV (AUROC, 0.906; 95% CI, 0.895–0.917) in HD-16; and across 0.83 mV (AUROC, 0.917; 95% CI, 0.911–0.924), along 0.46 mV (AUROC, 0.890; 95% CI, 0.883–0.897), north-east direction 0.89 mV (AUROC, 0.923; 95% CI, 0.917–0.929), and south-east direction 0.83 mV (AUROC, 0.913; 95% CI, 0.906–0.920) in HD-32. Significant differences in AUROC were seen between HD-16 along versus across ($P=0.002$), HD-16 north-east direction versus south-east direction ($P=0.01$), HD-32 north-east direction versus south-east direction ($P<0.0001$), and HD-16 along versus HD-32 along ($P=0.006$). The AUROC was significantly larger ($P<0.01$) when only the best points on each given site were selected for analysis, compared with when all points were used.

CONCLUSIONS: Spacing and orientation of bipoles impacts the accuracy of scar detection. Optimal threshold specific to each bipolar configuration should be determined. Selecting one best voltage point among multiple points projected on the same surface is also critical on the Ensite-system to increase the accuracy of scar-mapping.

VISUAL OVERVIEW: A [visual overview](#) is available for this article.

Masateru Takigawa, MD, PhD*
Jatin Relan, MD, PhD*
et al

*Drs Takigawa and Relan contributed equally to this work.

The full author list is available on page 10.

Key Words: arrhythmia ■ electrophysiology ■ magnetic resonance spectroscopy ■ myocardial infarction ■ sheep ■ tachycardia ventricular

© 2019 American Heart Association, Inc.

<https://www.ahajournals.org/journal/circep>



WHAT IS KNOWN?

- Areas with the voltage between 0.5 and 1.5 mV have been defined as abnormal low voltage areas. However, these thresholds may be dependent on the electrode spacing and the angle between bipolar direction and activation direction.

WHAT THE STUDY ADDS?

- Optimal cutoff value to discriminate scar from healthy tissue is specific to bipolar spacing and orientation.
- Although scar areas are well discriminated from the healthy area in any bipolar configurations with the HD-grid catheter (Advisor) with both a sensitivity and specificity of 80% to 85%, smallest bipolar spacing (1 mm) showed relatively lower accuracy.
- Selecting the best point out of multiple points projected on the same given site may provide better accuracy to discriminate scar.

Detection and characterization of myocardial scar is a prerequisite for substrate-based scar modification during sinus rhythm as mapping during ventricular tachycardia (VT) can be performed in only 30% to 40% of cases.^{1,2} Bipolar voltage mapping has been correlated with dense scar defined by histopathology and magnetic resonance imaging (MRI) and has been universally implemented in clinical practice, with a statistically derived low voltage threshold of <1.5 mV.^{3,4} However, not only electrode size and spacing,^{5–7} but also the activation wavefront relative to the catheter orientation, influence the local voltage.^{8–10}

The purpose of this study was to explore the optimal threshold in 2 configurations of HD-grid catheters (Figure 1), and compare the impact of electrode spacing and bipolar direction on the scar-threshold. Additionally, we aimed to assess the feature of best-duplicated point installed in the EnSite Precision system, which automatically selects the highest voltage point among multiple points projected on the same surface point to create more accurate maps.

METHODS

The data, methods used in the analysis, and materials used to conduct the research will not be made available for purposes of reproducing the results or replicating the procedure.

Animal Model for Myocardial Infarction

Experimental protocols were conducted in compliance with the Guiding Principles in the Use and Care of Animals published by the National Institutes of Health (NIH Publication No. 85-23, Revised 1996). The study was approved by the institutional animal use and care committee. Six female sheep (age 4.5 years, 55.4±7.3 kg) were sedated with an intramuscular injection of

ketamine hydrochloride (20 mg/kg), acepromazine (0.1 mg/kg), and buprenorphine (20 µg/kg). After an intravenous injection of propofol (2 mg/kg), each sheep was intubated, and anesthesia was maintained with 2% to 3% isoflurane. Sheep were ventilated with a respirator (CARESTATION/Carescape GE, Chicago), using room air supplemented with oxygen. An intravenous catheter was placed in the internal jugular vein for infusion of drugs and fluids. Arterial blood gases were monitored periodically, and ventilator parameters were adjusted to maintain blood gases within physiological ranges. A sheep myocardial infarction model was created by an experienced invasive cardiologist using selective ethanol injection (1–2 cc) in the distal one-third of the left anterior descending artery.

MRI Myocardial Scar Segmentation

Late gadolinium-enhanced cardiac MRI was performed 2 to 3 months after the creation of myocardial infarction. Image processing was performed by 2 trained technicians using the MUSIC software (EQUIPEX MUSIC, Liryc, Université de Bordeaux/INRIA, Sophia Antipolis, France). Segmentation was performed as described previously.¹¹ Briefly, the cardiac chambers, ventricular epicardium, ascending aorta, and coronary sinus were segmented using semi-automatic methods.¹¹ Although adaptive histogram thresholding was applied to segment dense scar (threshold set at 50% maximum signal intensity) and gray zone (from 35%–50%)^{12–14} from left ventricular wall segmentation, these regions were all defined as scar areas in the present study.

Electrophysiological Study and Mapping With HD-32 Grid Catheter

An electrophysiological study for scar mapping was performed 1 to 3 days after the MRI examination in surviving post-infarct sheep, using the HD-32 Grid catheter (Abbott, Minneapolis, MN) and 3D-electroanatomical mapping system (EnSite Precision system, Research version, Abbott, Minneapolis, MN), with identical sedation, analgesia, intubation and ventilation protocols as previously. A quadripolar diagnostic catheter (Inquiry, Abbott, Minneapolis, MN) was placed in the right ventricle, inferior vena cava, and coronary sinus. A quadripolar positioned at the level of the inferior vena cava was used as the reference catheter for unipolar electrograms. The left ventricular was mapped during sinus rhythm with the HD-32 Grid catheter (3 mm inter-electrode spacing and 1 mm electrode size) via a retrograde aortic approach and trans-septal approach. Multiple bipolar configurations were created as described in the following paragraph. A steerable long sheath (Agilis, Abbott, Minneapolis, MN) was used if required. The internal and external projection setting was set at 5 mm with 5 mm interpolation. Field-scaling was applied for all maps. On the point acquisition, contact with the left ventricular endocardial surface was confirmed by fluoroscopy and the proximity indicator on the EnSite Precision system.

For the registration, all segmentations of MRI imaging, including scar and healthy areas, were exported as meshes and loaded into the EnSite Precision system. The registration algorithm with the EnSite-NavX Fusion module allowed dynamic molding of the 3D-electroanatomical mapping

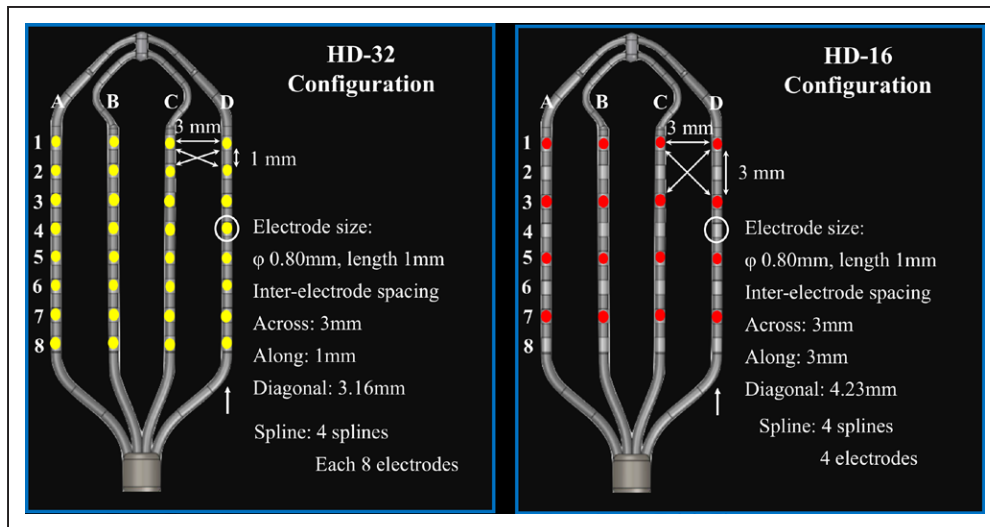


Figure 1. Bipolar configuration from the HD-32 Grid catheter.

A, All electrodes were used for HD-32 Grid catheter. Electrocardiograms (EGMs) were collected from along (eg, A1-A2, A2-A3...D7-D8), across (eg, A1-B1, B1-C1, C1-D1, A2-B2, B2-C2...C8-D8), north-east diagonal (eg, A2-B1, B2-C1, C2-D1...C8-D7), and south-east diagonal (eg, A1-B2, B1-C2, C1-D2...C7-D8) electrodes. **B**, Every other electrode on each spline is skipped to produce a HD-16 configuration, which is simulating the Advisor HD-Grid mapping catheter (Abbott, Minneapolis, MN). EGMs are collected from along (eg, A1-A3, A3-A5...D7-D8), across (eg, A1-B1, B1-C1, C1-D1, A3-B3, B3-C3...C7-D7), north-east diagonal (eg, A3-B1, B3-C1, C3-D1...C7-D5), and south-east diagonal (eg, A1-B3, B1-C3, C1-D3...C5-D7) electrodes.

geometry onto the MRI surface.¹⁵ After primary registration, the registered model was refined using a second set of fiducial points, for example, left atrium, coronary sinus, aortic root, left ventricular apex, and mitral annulus, judiciously placed in a stepwise fashion to further align both surfaces at sites of local mismatch.

Bipolar Configurations and Electrogram Analysis

With the HD-32 Grid catheter, an electrode pair can be selected to create a bipolar electrogram. By skipping every other electrode, electrograms with a HD-16 Grid configuration, which is similar to that of the Advisor HD-Grid mapping catheter (Abbott, Minneapolis, MN), were also simulated in each acquired beat, as shown in Figure 1. Electrograms were classified as MRI-defined scar or nonscar areas and used for further analysis (Figure 2). Using the research version of EnSite Precision system, the absolute distance of each mapped point from the surface geometry was calculated. All points within 5 mm from the surface were included in the study. As well as unipolar electrograms, bipolar electrograms were acquired from electrode pairs along to the catheter shaft (eg, A1-A2, A2-A3 etc for the HD-32-Grid, and A1-A3, A3-A5 etc for the HD-16-Grid), across to the catheter shaft (A1-B1, B1-C1 etc for both HD-32-Grid and HD-16-Grid), and diagonal directions (north-east [NE] and south-east [SE]; A1-B2, B1-A2 etc for the HD-32-Grid, and A1-B3, B1-A3 etc for the HD-16-Grid). Electrograms acquired from a distorted catheter and those with noise or artifacts were excluded. Unipolar and bipolar electrograms were filtered from 2 to 100 Hz, and 30 to 300 Hz, respectively and local voltages were automatically analyzed from peak-to-peak voltages.

The optimal cutoff value of the local voltage and the predictive accuracy for scar identification was calculated based

on the receiver operating characteristic (ROC) analysis. The same analysis was then performed using only best duplicated points, one of the default settings of EnSite Precision system, in which the electrogram with the highest amplitude is selected as a local electrogram when multiple points are projected on the same surface to create the voltage map. The optimal cutoff value and predictive accuracy were compared with the values calculated using all points (<5 mm from the surface).

Statistical Analysis

For continuous variables, data are expressed as mean (\pm SD) when they follow a normal distribution; or as median (25th percentile–75th percentile) if they do not. As a result, the former was used to describe the area under the ROC curve (AUROC), and the latter was applied to describe the voltages. Spearman correlation coefficient was also calculated. For categorical variables, data are described as numbers and percentages. According to the skewness, χ^2 analysis or Fisher's exact test were used for categorical variables, and an ANOVA analysis or Kruskal-Wallis test were used for continuous variables. *P* values <0.05 were considered statistically significant. To compare the diagnostic capability of each method, we performed a 2-sided Student *t* test on the mean \pm SD of each area under curve calculated, with the approximation of their normal distribution. The optimal cutoff value to detect the MRI-defined scar was based on the Youden's Index.

RESULTS

Electrogram Acquisition

Electrograms were successfully collected in sinus rhythm from a total of 456 acquisition sites (mean 76 \pm 12 per

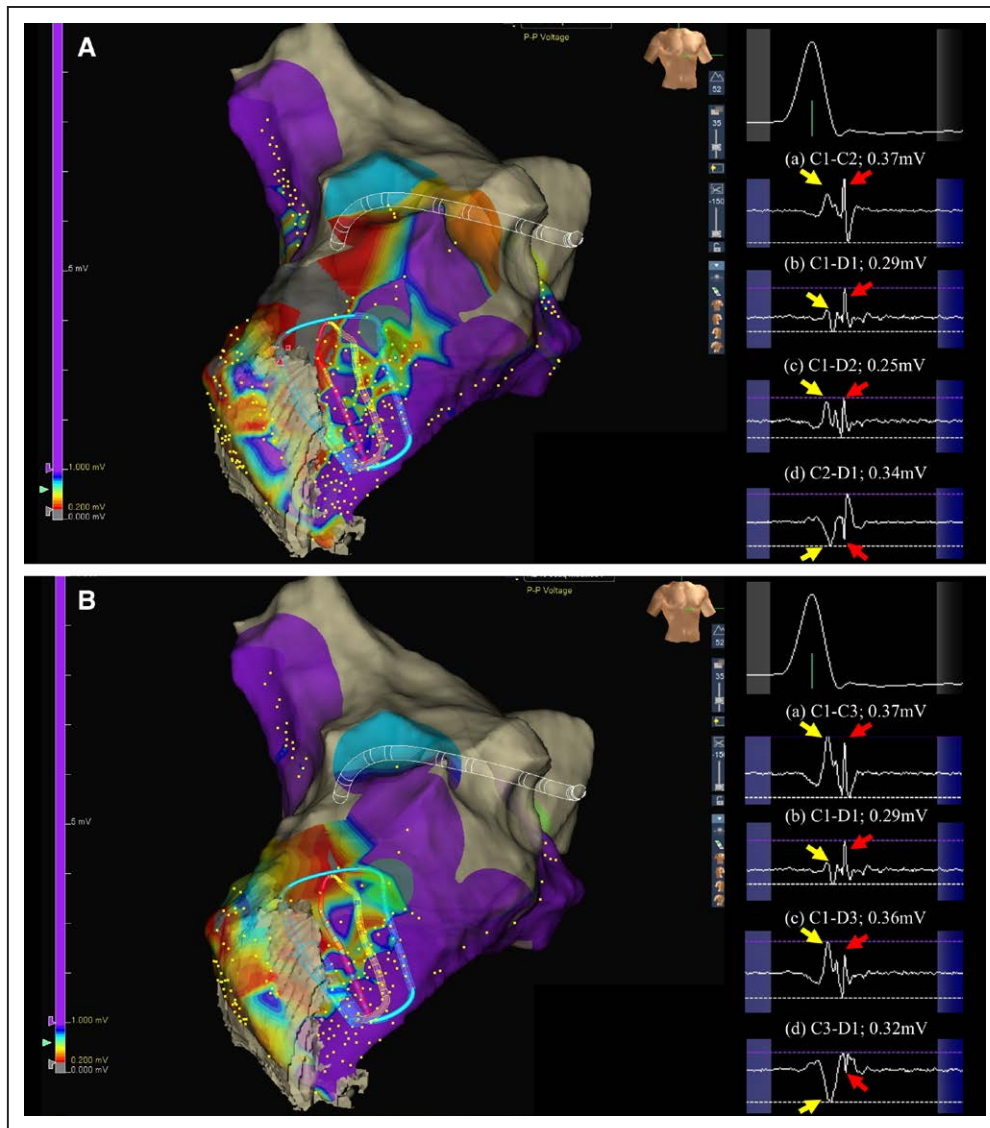


Figure 2. Collecting electrocardiograms (EGMs) with both HD-32 and HD-16 configurations from the same acquisitions.

The magnetic resonance imaging (MRI)–image with MRI-defined scar is merged on the 3D mapping system. From one acquisition, 4 EGMs are collected from both HD-32 (A) and HD-16 (B), allocated to MRI-defined scar and nonscar areas, and used for the analysis. Local voltages automatically calculated from peak-to-peak voltages consist in the combination of far- (yellow arrows) and near-field (red arrows) components. Note that far-field components in HD-16 are larger than HD-32 (a, c, d). However, near-field components are not always the case; larger in HD-32 (a, d) but smaller in HD-16 (c).

case) in prepared 6 infarcted sheep as shown in Table 1. Mapped points >5 mm further from the surface geometry or those with noise or artifact were excluded from the analysis. Five thousand five hundred fifty-four points with the HD-16 configuration and 10998 points with the HD-32 configuration for unipolar electrograms, and 14750 points with the HD-16 configuration and 32286 points with the HD-32 configuration for bipolar electrograms were analyzed.

Unipolar Voltages

As unipolar voltages, 3337 points in healthy areas and 2217 points in scar areas with the HD-16 configuration, and 6687 points in healthy areas and 4311 points

in scar areas with the HD-32 were analyzed (Table 2). There were no differences in unipolar voltage between HD-16 and HD-32 configurations in either healthy or scar areas ($P=N.S.$).

Table 1. Baseline Characteristics (N=6)

Sheep No.	Sex	Age, y	Weight, kg	Total Acquisitions
1	f	5	60	95
2	f	5	56.5	81
3	f	5	60	75
4	f	5	48	61
5	f	5	63	77
6	f	2	45	67

Table 2. Unipolar Voltages in Healthy and Scar Areas

	No. of Points	Unipolar Voltage, mV
Healthy		
HD-16	3337	5.62 [4.13–7.07]
HD-32	6687	5.63 [4.15–7.11]
Scar		
HD-16	2217	3.98 [3.12–4.56]
HD-32	4311	3.99 [3.12–4.56]

Bipolar Voltages

As bipolar voltages, 8950 points in healthy areas and 5800 points in scar areas with the HD-16 configuration, and 19882 points in healthy areas and 12415 points in scar areas with the HD-32 configuration were analyzed. Median voltages in different configurations are given in Table 3 for the HD-16 configuration and in Table 4 for the HD-32 configuration.

Effect of Electrode Spacing and Orientation

The direct effect of electrode spacing independent of direction is reflected by the difference in median voltage between the HD-32 along (1 mm spacing) and HD-16 along bipolar electrograms (3 mm spacing) Table 5. Median voltages were significantly larger with 3 mm spacing in both healthy and scar areas ($P < 0.0001$).

The direct effect of electrode direction independent of spacing is reflected by the difference in median voltage between along versus across bipolar electrograms in the HD-16, and NE versus SE bipolar electrograms in HD-16 and HD-32 configurations. In the scar areas, although the impact of bipolar orientation was not significant in 3 mm electrode spacing, it became significant when the inter-electrode spacing became larger

Table 3. Bipolar Voltages With HD-16 Grid in Healthy and Scar Areas

Bipolar Configuration (Inter-Electrode Spacing)	No. of points	Bipolar Voltage, mV
Healthy		
Across (3 mm)	2584	1.89 [1.13–3.00]
Along (3 mm)	2483	1.74 [1.00–2.87]
NE (4.23 mm)	1958	2.16 [1.28–3.34]
SE (4.23 mm)	1925	2.09 [1.31–3.24]
Scar		
Across (3 mm)	1635	0.35 [0.23–0.60]
Along (3 mm)	1727	0.34 [0.21–0.60]
NE (4.23 mm)	1165	0.41 [0.27–0.64]
SE (4.23 mm)	1273	0.49 [0.33–0.79]

NE indicates north-east; and SE, south-east.

Table 4. Bipolar Voltages With HD-32 Grid in Healthy and Scar Areas

Bipolar Configuration (Inter-Electrode Spacing)	No. of Points	Bipolar Voltage, mV
Healthy		
Across (3 mm)	5151	1.88 [1.11–3.03]
Along (1 mm)	5805	1.18 [0.57–2.14]
NE (3.16 mm)	4492	2.00 [1.15–3.19]
SE (3.16 mm)	4434	1.94 [1.16–3.13]
Scar		
Across (3 mm)	3176	0.35 [0.23–0.61]
Along (1 mm)	3796	0.19 [0.12–0.37]
NE (3.16 mm)	2679	0.36 [0.24–0.59]
SE (3.16 mm)	2764	0.40 [0.27–0.68]

NE indicates north-east; and SE, south-east.

and reached a 20% difference when the inter-electrode spacing was 4.23 mm, as shown in Table 5.

Optimal Cutoff Values

Optimal cutoff values to discriminate scar from healthy areas were determined using ROC analysis and are described in Tables 6 through 8. For unipolar HD16 electrograms, a cutoff voltage value of 4.91 mV was found (sensitivity 84.3%, specificity 61.2%), which did not change even when analyzed points were increased using points acquired with the HD-32 configuration (Table 6). These 2 configurations showed generally weaker spearman correlation ($\rho < 0.5$) compared with bipolar configurations. For bipolar voltages, the optimal cutoff voltage value and the AUROC differed depending on spacing and the orientation of bipoles; across 0.84 mV (AUROC, 0.920; 95% CI, 0.911–0.928), along 0.76 mV (AUROC, 0.903; 95% CI, 0.893–0.912), NE 0.95 mV (AUROC, 0.923; 95% CI, 0.913–0.932), and SE 0.87 mV (AUROC, 0.906; 95% CI, 0.895–0.917) in HD-16; and across 0.83 mV (AUROC, 0.917; 95% CI, 0.911–0.924), along 0.46 mV (AUROC, 0.890; 95% CI, 0.883–0.897), NE 0.89 mV (AUROC, 0.923; 95% CI, 0.917–0.924), and SE 0.83 mV (AUROC, 0.913; 95% CI, 0.906–0.920) in HD-32. When we focused on the spacing, the optimal cutoff voltage values and AUROCs were as follows: 1 mm spacing 0.46 mV (AUROC, 0.890; 95% CI, 0.883–0.897), 3 mm spacing 0.80 mV (AUROC, 0.912; 95% CI, 0.907–0.918), 3.16 mm spacing 0.89 mV (AUROC, 0.918; 95% CI, 0.913–0.922) and 4.23 mm spacing 0.90 mV (AUROC, 0.913; 95% CI, 0.906–0.921). A strong spearman correlation ($\rho \geq 0.7$) was obtained regardless of bipolar configurations. Although relatively high accuracy and reliability was preserved in all bipolar configurations, significant differences were observed between settings as shown in Table in the [Data Supplement](#).

Table 5. Direct Voltage Comparison Based on Electrode Spacing and Orientation

	Voltage in Healthy Areas, mV	P Values	Voltage in Scar Areas, mV	P Values
Comparison of spacing				
HD-16 along vs. HD-32 along (3 mm vs. 1 mm spacing)	1.74 [1.00–2.87] vs 1.18 [0.57–2.14]	<0.0001	0.34 [0.21–0.60] vs 0.19 [0.12–0.37]	<0.0001
Comparison of orientation				
HD-16 across vs HD-16 along (3 mm spacing)	1.89 [1.13–3.00] vs 1.74 [1.00–2.87]	0.002	0.35 [0.23–0.60] vs 0.34 [0.21–0.60]	0.2
HD-32 NE vs HD-32 SE (3.16 mm spacing)	2.00 [1.15–3.19] vs 1.94 [1.16–3.13]	0.35	0.36 [0.24–0.59] vs 0.40 [0.27–0.68]	<0.0001
HD-16 NE vs HD-16 SE (4.23 mm spacing)	2.16 [1.28–3.34] vs 2.09 [1.31–3.24]	0.76	0.41 [0.27–0.64] vs 0.49 [0.33–0.79]	<0.0001

NE indicates north-east; and SE, south-east.

Specifically, the HD-32 along configuration (1 mm spacing) showed significantly higher AUROC values than in the HD-32 across configuration (3 mm spacing; $P<0.001$), and the HD-16 along (3 mm spacing; $P=0.006$). Additionally, significant difference in AUROC was observed between 1 mm spacing versus 3 mm, 3.16 mm and 4.23 mm spacing ($P<0.001$); HD-32 along configuration (1 mm spacing) demonstrated a weaker spearman correlation, showing a lower reliability.

ages, the optimal cutoff voltage value differed depending on spacing and the orientation of the bipoles as follows: across 0.99 mV, along 1.01 mV, NE 1.17 mV, and SE 1.16 mV in HD-16; and across 0.90 mV, along 0.84 mV, NE 1.18 mV, and SE 1.02 mV in HD-32. Both the AUROC and Spearman correlation were generally significantly larger when only the best points on each given site were selected for analysis compared with when all points were used for analysis, as shown in Table 8.

All Points Versus Selected Points Among Multiple Duplicated Points

When only selected points (those with the largest voltage) were used instead of all points for analysis, the optimal cutoff unipolar values for HD-16 and HD-32 were 4.85 mV and 5.01 mV, respectively (Table 7). For bipolar volt-

DISCUSSION

Major Findings

In the present study, we examine the impact of bipolar spacing and orientation on the scar threshold and demonstrate the following.

Table 6. Optimal Cutoff Value Based on All Acquired Points

	Analyzed Points	Optimal Cutoff Voltage, mV	AUROC (95% CI)	Sensitivity, %	Specificity, %	Spearman Correlation, ρ
HD16						
Unipolar	5554	4.91	0.741 (0.728–0.755)	84.3	61.2	0.410*
Across (3 mm)	4219	0.84	0.920 (0.911–0.928)	84.9	85.2	0.709*
Along (3 mm)	4210	0.76	0.903 (0.893–0.912)	81.8	83.2	0.686*
NE (4.23 mm)	3123	0.95	0.923 (0.913–0.932)	86.0	84.9	0.708*
SE (4.23 mm)	3198	0.87	0.906 (0.895–0.917)	78.6	88.2	0.688*
HD-32						
Unipolar	10998	4.89	0.745 (0.739–0.754)	83.7	62.1	0.414*
Across (3 mm)	8327	0.83	0.917 (0.911–0.924)	84.5	85.3	0.702*
Along (1 mm)	9601	0.46	0.890 (0.883–0.897)	81.2	81.3	0.660*
NE (3.16 mm)	7171	0.89	0.923 (0.917–0.929)	86.3	84.2	0.709*
SE (3.16 mm)	7187	0.83	0.913 (0.906–0.920)	82.2	86.6	0.695*
Independent of orientation						
3 mm	12537	0.80	0.912 (0.907–0.918)	83.4	84.6	0.700*
3.16 mm	14358	0.85	0.918 (0.913–0.922)	83.9	85.5	0.702*
4.23 mm	6321	0.90	0.913 (0.906–0.921)	82.0	86.6	0.697*

AUROC indicates area under the ROC curve; NE, north-east; and SE, south-east.

* $P<0.001$

Table 7. Optimal Cutoff Values Based on Selected Points

	Analyzed Points	Optimal Cutoff Voltage, mV	AUROC (95% CI)	Sensitivity, %	Specificity, %	Spearman Correlation, ρ
HD16						
Unipolar	3930	4.85	0.791 (0.777–0.806)	88.4	65.3	0.494*
Across (3 mm)	695	0.99	0.931 (0.911–0.951)	83.8	88.7	0.674*
Along (3 mm)	1028	1.01	0.946 (0.932–0.960)	90.4	86.1	0.723*
NE (4.23 mm)	771	1.17	0.955 (0.940–0.970)	89.9	89.5	0.750*
SE (4.23 mm)	761	1.16	0.938 (0.921–0.955)	87.7	86.8	0.748*
HD-32						
Unipolar	5284	5.01	0.823 (0.811–0.834)	89.5	70.1	0.553*
Across (3 mm)	840	0.90	0.943 (0.927–0.958)	82.9	92.7	0.716*
Along (1 mm)	1167	0.84	0.909 (0.892–0.926)	84.8	80.8	0.658*
NE (3.16 mm)	1071	1.18	0.963 (0.953–0.974)	94.5	88.6	0.759*
SE (3.16 mm)	1101	1.02	0.928 (0.912–0.943)	87.7	86.8	0.718*
Independent of orientation						
3 mm	1868	1.01	0.944 (0.933–0.955)	87.7	87.6	0.707*
3.16 mm	2171	1.06	0.946 (0.937–0.956)	90.9	87.4	0.741*
4.23 mm	1532	1.16	0.947 (0.935–0.958)	88.3	88.4	0.751*

AUROC indicates area under the ROC curve; NE, north-east; and SE, south-east.
* $P < 0.001$.

Using high-density mapping:

1. Bipolar voltage increases as the inter-electrode spacing increases in both healthy and scar tissue.
2. In scar areas, bipolar orientation may impact the voltage, particularly when the bipolar spacing is larger.
3. Optimal cutoff value to discriminate scar from healthy tissue is specific to bipolar spacing and orientation.
4. Smallest bipolar spacing (1 mm) less effectively discriminate scar from healthy tissue.
5. Selecting the best point out of multiple points projected on the same given site may provide better accuracy to discriminate scar.

The Impact of the Bipolar Spacing on the Local Voltage and Scar Threshold

Our results demonstrate that bipolar voltages generally increase as the inter-electrode spacing increases in both healthy and scar areas. Excluding the effect of wavefront direction by comparing HD-16 along (3 mm spacing) versus HD-32 along (1 mm spacing), resulted in a remarkable difference. Although each bipolar configuration provided high sensitivity and specificity of $\approx 80\%$ to 85% in discriminating scar from healthy tissue, with an optimal cutoff value for each bipolar setting, the smallest spacing (1 mm) seemed to be less accurate. This unexpected result may be explained by the fact that local voltages in the scar areas were more heterogeneous, with both far-field and near-field voltages

measured from the electrodes with smaller spacing. As previously demonstrated, far-field components increase more proportionally increase as the spacing increases, while near-field components are more sensitive to the local tissue and exaggerated in smaller electrode spacing.⁷ As a result, far- and near-field voltages may be more frequently overlapped with smaller spacing, while, probably in bipoles with larger spacing, local

Table 8. Comparison of the AUROC Between All-Point Analysis Versus Selected Point Analysis

	All Points	Selected Points (Largest Voltage)	P Values
HD16			
Unipolar	0.741 \pm 0.007	0.791 \pm 0.007	<0.001
Across (3 mm)	0.920 \pm 0.004	0.931 \pm 0.100	0.31
Along (3 mm)	0.903 \pm 0.005	0.946 \pm 0.007	<0.001
NE (4.23 mm)	0.923 \pm 0.005	0.955 \pm 0.007	0.003
SE (4.23 mm)	0.906 \pm 0.006	0.938 \pm 0.009	0.004
HD-32			
Unipolar	0.745 \pm 0.005	0.823 \pm 0.006	<0.001
Across (3 mm)	0.917 \pm 0.003	0.943 \pm 0.008	0.004
Along (1 mm)	0.890 \pm 0.003	0.909 \pm 0.009	0.01
NE (3.16 mm)	0.923 \pm 0.003	0.963 \pm 0.005	<0.001
SE (3.16 mm)	0.913 \pm 0.004	0.928 \pm 0.008	0.065
Independent of orientation			
3 mm spacing	0.912 \pm 0.003	0.944 \pm 0.005	<0.001
3.16 mm spacing	0.918 \pm 0.002	0.946 \pm 0.005	<0.001
4.23 mm spacing	0.913 \pm 0.004	0.947 \pm 0.006	<0.001

voltages were more uniformly measured from the larger far-field components in scar areas as described in a previous study.¹⁶

The effect of spacing on the optimal cutoff values has been elegantly described by Tung et al.¹⁷ They demonstrate an increasing linear relationship between optimal voltage thresholds for scar and wider bipolar spacing. In their study, the optimal cutoff value with a duo-decapolar catheter (1 mm electrode length and 2 mm spacing) was 6.7 mV for unipolar, and 2.02 mV for bipolar configurations. Interestingly, optimal cutoff values of both unipolar- and bipolar-voltages with the HD-16 configuration were 4.91 mV and 0.76 to 0.84 mV in the present study, much smaller than in Tung's report, even though the electrode length was the same (1 mm) and the HD-16 inter-electrode spacing was larger. One reason for this discrepancy may originate from the difference of the electrode surface area, as this is $\approx 3\times$ larger in the duo-decapolar catheter, impacting the voltage threshold due to a larger far-field effect. This may also suggest a larger contribution from far-field signal component with larger surface electrodes. Regarding inter-electrode spacing, the commercially available HD-grid catheter (Advisor) may provide a larger voltage (with a greater far-field effect) than other commercially available multipolar mapping catheters due to a larger inter-electrode spacing. However, other factors affecting electrograms, such as electrode size and surface area should be acknowledged.

Interestingly, as theoretically expected, the present study demonstrated that the optimal cutoff value for unipolar voltage was similar between HD-16 and HD-32, because the electrode size was the same between these 2 configurations even though a larger number of points was collected for the HD-32.

The Impact of the Orientation of Bipolar Pair on the Local Voltage and Scar Threshold

The angle between the bipolar orientation and activation front has been reported to affect local voltages.^{8–10} In scar areas, propagation may vary even more widely, due to the heterogeneity between fibrous tissue and interposed surviving myocardial fibers. In addition, a greater available mass of normal far-field myocardium contributes to the local bipolar electrograms in the border area adjacent to the healthy muscle, resulting in a combination of near-field and far-field electrograms. Peak-to-peak voltages in these areas showed $\approx 30\%$ to 35% variation between orthogonally diagonal bipolar pairs at the same location.⁹ Although this effect may have been nullified by adding mapping data from other catheter orientations, we still observed that the impact of bipole orientation in scar areas was exaggerated when the bipolar spacing was larger, as shown in

Table 5. As far-field components are usually exaggerated with larger inter-electrode spacing,⁷ this finding may be linked to the relation between far-field voltage versus activation direction in scar areas. Since the present study did not show a significant difference between orthogonal bipolar directions for the 3 mm spacing, a smaller inter-electrode spacing may offset the impact of this far-field effect associated with overall activation direction. However, this should be confirmed by using bipoles with much smaller spacing. Additionally, the clinical impact of the limited difference ($\approx 20\%$) should be examined in clinical studies using an ablation strategy based on these different cutoff values.

The Impact of Selecting the Best Points in the Projected Location

The present study demonstrated that the optimal cutoff values calculated from selected points on each projected site provided a higher accuracy for scar discrimination compared with those calculated from all acquired points. Although high-density mapping with a multipolar mapping catheter can display substrate with higher spatial resolution, multiple points may be deleterious as they may not provide the true voltage at each given site due to orientation of bipoles versus activation direction.

However, one possible important limitation to this function is that by selecting the highest amplitude signal, it may favor far-field components over the near-field ones, and therefore reduce the ability to display the local abnormal ventricular activities in the scar⁷ (Figure 3), and this limitation is critical for the recent approaches of VT substrate ablation.^{18–22} Additionally, the gap on the linear lesion may be missed by a voltage map when double potentials with large far-field components are identified along the linear lesion.

Scar Threshold in Commercially Used Catheter

The findings of the present study suggest that in the EnSite Precision system with the Advisor HD-Grid Mapping Catheter using the best points option, the threshold of 4.85 mV in unipolar voltage and 1.01 mV in bipolar voltage (3 mm along bipoles) may be used for scar detection. However, the value derived from the animal data maybe not always applicable to the human data.

Recently, industry has provided several types of multipolar mapping catheters with different electrode size and inter-electrode spacing. Compared with the Advisor (3 mm inter-electrode spacing, 1 mm electrode length, surface area of 2.51 mm²), the PentaRay (Biosense-Webster Inc, Diamond Bar, CA) has a smaller inter-electrode spacing (2 mm) and similar electrode length (1 mm) but larger surface area (3.14 mm²). The

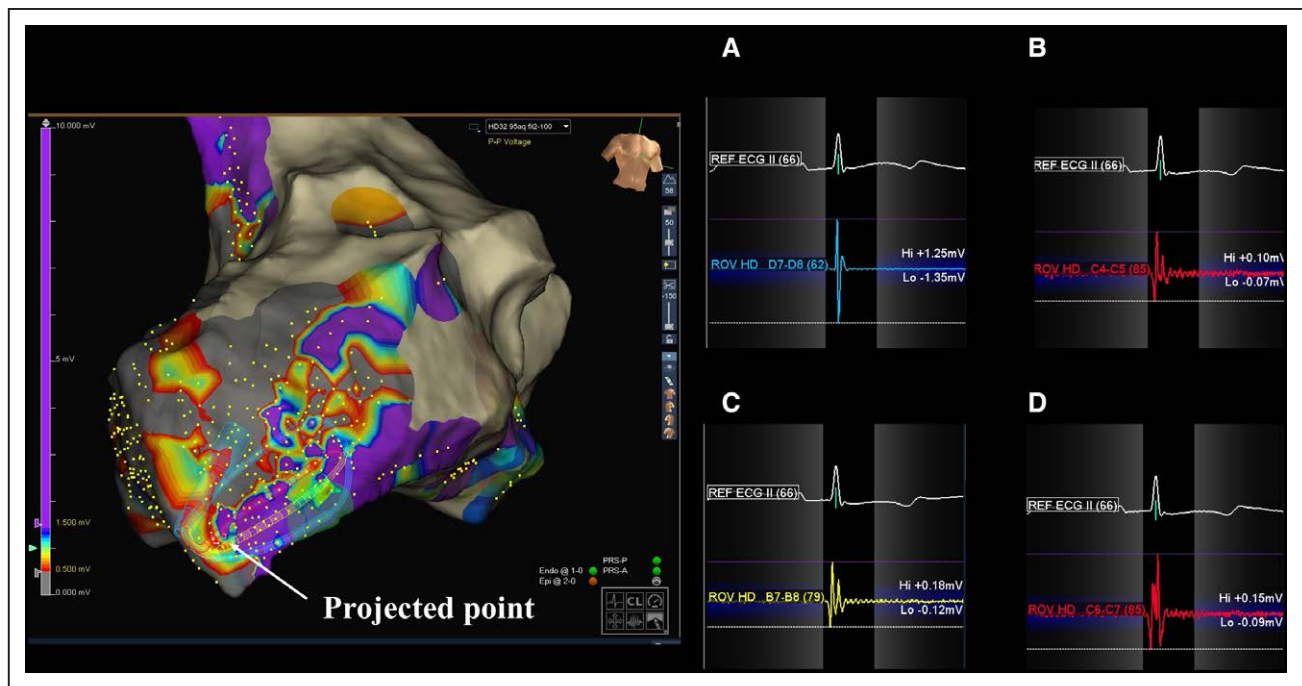


Figure 3. Examples of best electrocardiograms (EGMs) selected out of multiple EGMs projected on a given site.

In the scar border area, 4 duplicated points (A–D) are projected on the same surface point, (A) with the highest amplitude selected as the local voltage to create the voltage map. Although, EGMs at (B–D) depict local abnormal ventricular activities, this is not reflected on the map. Catheter is placed on a similar region but with a different acquisition and with a different angle. These adjacent points are projected on the same surface, and one of them with a highest voltage is picked up as a local voltage with a default setting of the commercial version of the NavX precision system, which results in missing a local abnormal EGMs. This situation more frequently happens on the scar border areas.

Orion (Boston Scientific, Marlborough, MA) has a smaller inter-electrode spacing (2.5 mm) and much smaller electrode size (0.4 mm²). Although bipolar voltages and local resolution are affected not only by the inter-electrode spacing, but also the electrode size (and not just electrode length), a direct comparison may be required to decide on superiority between these catheters. However, at the least, a threshold for scar detection should be set for each catheter. Since the commercially used HD-16 (Advisor) has a relatively large inter-electrode spacing, the resolution may be worse than for other multipolar mapping catheters. However, using multiple bipolar configurations may increase the resolution, and the detection of abnormal potentials such as local abnormal ventricular activities may be improved, and the sequential arrangement of electrodes may allow us to easily observe activation direction. However, this should be analyzed in a further study.

One Voltage Threshold or 2 Voltage Thresholds

Although we have been using 2 cutoff values for scar determination, this may not always be relevant to the clinical ablation strategy. First, although several strategies for VT substrate modification have been reported with good results,^{18–22} distinguishing the so-called dense scar (<0.5 mV) from border area (0.5–1.5 mV) does not

help identifying critical electrograms/isthmuses as they can be found in both. This means that identification of the entire scar area may be more important than discrimination of dense scar.

Second, a value of <0.5 mV as dense scar has been previously determined through intraoperative mapping using an ablation catheter in patients with postinfarction VT.²³ Additionally, a value of ≥ 1.5 mV as healthy tissue is based on voltage mapping from the normal heart in the absence of structural disease, and the voltage between 0.5 mV and 1.5 mV defined as abnormal low voltage areas.⁴ However, dense scar does not mean the absence of residual myocyte bundles in these areas. The residual tissue inside scar generally provides low voltage and high-frequency electrograms represented by local near-field electrograms,²² which may be critical to VT circuits. However, mapping system will automatically consider the voltage of the largest electrogram, which most often is not the critical one, being the far-field component.¹⁶ Since there are huge overlaps of voltage values between residual surviving tissue and far-field electrograms from healthy tissue in the dense scar area (<0.5 mV), identifying truly dead scar may not be simple or feasible. Smaller electrodes with smaller inter-electrode spacing minimize the far-field effect and probably more frequently collect near-field components, but still not able to avoid overlap.^{7,16}

Clinical Implications

Larger inter-electrode spacing providing larger bipolar voltage values in both healthy and scar areas. Bipolar orientation affects local voltage and may not be completely set off by catheter manipulation, which certainly highlights the interest of omnipolar mapping.²⁴

Although voltage thresholds for scar detection are specific to the electrode configuration, the accuracy of discriminating scars from healthy tissue is generally high with high-density mapping using the HD-grid as described by the AUROC=0.9. Smaller spacing (1 mm) does not better discriminate scar areas from healthy areas than larger spacing, but may be superior in identifying local signal from surviving bundles in the scar. Finally, voltage detection of scar is improved by using the best voltage points. However, we have to emphasize that our results do not mean that smaller spacing is inferior to larger spacing in investigating critical electrograms for VT-substrate such as local abnormal ventricular activities. Local abnormal ventricular activities detection has been shown to be superior with smaller inter-electrode spacing⁷ and multiple bipolar orientations.^{9,24}

LIMITATIONS

First, the small number of animals is a significant limitation in this study. Additionally, this animal model is likely different from that seen in patients with post-myocardial infarction. The infarct produced in sheep is more homogeneous, with smaller border zone, for example. Therefore, the applicability of the cutoff values in the present study must be cautiously examined in human studies. However, it is useful to describe the impact of spacing and orientation on scar characterization, and that the accuracy is relatively highly preserved in high-density mapping with the HD-grid catheter when specific cutoff values are used. It is also important to acknowledge that the local electrogram amplitude is measured based on the peak-to-peak voltage which is automatically calculated by the system, that is, from mixed electrograms with far- and near-field components, especially in scar areas. It would have been interesting to have performed the study using different pacing vectors, which may form the basis for a further study. Finally, smaller inter-electrode spacing (1 mm along/1 mm across) may offset the effect of bipole orientation versus activation, but a catheter with such a design was not available.

CONCLUSIONS

Voltages in both scar and healthy areas are affected by the spacing and orientation of the bipolar electrode configuration. The threshold to discriminate scar (vs MRI) from healthy tissue should be specifically defined

according to the bipolar configuration, but relatively high accuracy is preserved in any bipolar configuration with HD-grid when the specific cutoff is used for each bipolar configuration. Automatically selecting the best point out of multiple points projected on the same given site may reduce redundant data and increase accuracy. Including bipolar orientation in mapping systems should be considered in the future.

ARTICLE INFORMATION

Received January 23, 2019; accepted July 2, 2019.

The Data Supplement is available at <https://www.ahajournals.org/doi/suppl/10.1161/CIRCEP.119.007158>.

Authors

Masateru Takigawa, MD, PhD*; Jatin Relan, MD, PhD*; Takeshi Kitamura, MD; Claire A. Martin, MD, PhD; Steven Kim, PhD; Ruairidh Martin, MD; Ghassen Cheniti, MD; Konstantinos Vlachos, MD, PhD; Grégoire Massoulié, MD; Antonio Frontera, MD; Nathaniel Thompson, MD; Michael Wolf, MD; Felix Bourier, MD, PhD; Anna Lam, MD; Josselin Duchateau, MD; Thomas Pambrun, MD; Arnaud Denis, MD; Nicolas Derval, MD; Xavier Pillois, PhD; Julie Magat, PhD; Jerome Naulin, MSc; Mathilde Merle, MSc; Florent Collot, MSc; Bruno Quesson, PhD; Hubert Cochet, MD, PhD; Méléze Hocini, MD, PhD; Michel Haïssaguerre, MD, PhD; Frederic Sacher, MD, PhD; Pierre Jaïs, MD, PhD

Affiliations

IHU Liryc, Electrophysiology and Heart Modeling Institute, Fondation Bordeaux Université, Bordeaux University Hospital (CHU), Electrophysiology and Ablation Unit, University of Bordeaux, Centre de recherche Cardio-Thoracique de Bordeaux, France/Pessac-Bordeaux, France (M.T., J.R., T.K., C.A.M., S.K., R.M., G.C., K.V., G.M., A.F., N.T., M.W., F.B., A.L., J.D., T.P., A.D., N.D., X.P., J.M., J.N., M.M., F.C., B.Q., H.C., M. Hocini, M. Haïssaguerre, F.S., P.J.). Heart Rhythm Center, Tokyo Medical and Dental University, Japan (M.T.). Abbott, Minneapolis, MN (J.R., S.K.). Royal Papworth Hospital, Cambridge (C.A.M.). Institute of Genetic Medicine, Newcastle University, United Kingdom (R.M.).

Correspondence

Masateru Takigawa, MD, PhD, IHU Liryc, Electrophysiology and Heart Modeling Institute, Fondation Bordeaux Université, Bordeaux University Hospital (CHU), Electrophysiology and Ablation Unit, University of Bordeaux, Centre de recherche Cardio-Thoracique de Bordeaux, Ave de Magellan, 33604 Bordeaux-Pessac, France. Email teru.takigawa@gmail.com

Sources of Funding

This study was funded by public funding Equipex MUSIC ANR-11-EQPX-0030 and IHU LIRYC ANR-10-IAHU-04.

Disclosures

Drs Haïssaguerre, Hocini, Jaïs, and Sacher have received lecture fees from Biosense Webster and Abbott. Drs Denis, Derval, Jaïs, and Sacher received speaking honoraria and consulting fees from Boston Scientific. Drs Relan and Kim are employees of Abbott. The other authors report no conflicts.

REFERENCES

1. Tung R, Vaseghi M, Frankel DS, Vergara P, Di Biase L, Nagashima K, Yu R, Vangala S, Tseng CH, Choi EK, Khurshid S, Patel M, Mathuria N, Nakahara S, Tzou WS, Sauer WH, Vakil K, Tedrow U, Burkhardt JD, Tholakanahalli VN, Saliaris A, Dickfeld T, Weiss JP, Bunch TJ, Reddy M, Kanmanthareddy A, Callans DJ, Lakkireddy D, Natale A, Marchlinski F, Stevenson WG, Della Bella P, Shivkumar K. Freedom from recurrent ventricular tachycardia after catheter ablation is associated with improved survival in patients with structural heart disease: an international VT ablation center collaborative Group study. *Heart Rhythm*. 2015;12:1997–2007. doi: 10.1016/j.hrthm.2015.05.036

2. Josephson ME. Electrophysiology of ventricular tachycardia: an historical perspective. *J Cardiovasc Electrophysiol*. 2003;14:1134–1148.
3. Callans DJ, Ren JF, Michele J, Marchlinski FE, Dillon SM. Electroanatomic left ventricular mapping in the porcine model of healed anterior myocardial infarction. Correlation with intracardiac echocardiography and pathological analysis. *Circulation*. 1999;100:1744–1750. doi: 10.1161/01.cir.100.16.1744
4. Marchlinski FE, Callans DJ, Gottlieb CD, Zado E. Linear ablation lesions for control of unmappable ventricular tachycardia in patients with ischemic and nonischemic cardiomyopathy. *Circulation*. 2000;101:1288–1296. doi: 10.1161/01.cir.101.11.1288
5. Anter E, Josephson ME. Substrate mapping for ventricular tachycardia. *JACC Clin Electrophysiol*. 2015;1:341–352.
6. Berte B, Relan J, Sacher F, Pillois X, Appetiti A, Yamashita S, Mahida S, Casassus F, Hooks D, Sellal JM, Amraoui S, Denis A, Derval N, Cochet H, Hocini M, Haïssaguerre M, Weerasooriya R, Jais P. Impact of electrode type on mapping of scar-related VT. *J Cardiovasc Electrophysiol*. 2015;26:1213–1223. doi: 10.1111/jce.12761
7. Takigawa M, Relan J, Martin R, Kim S, Kitamura T, Frontera A, Cheniti G, Vlachos K, Massoulié G, Martin CA, Bourier F, Lam A, Wolf M, Duchateau J, Klotz N, Pambrun T, Denis A, Derval N, Magat J, Naulin J, Merle M, Collot F, Quesson B, Cochet H, Hocini M, Haïssaguerre M, Sacher F, Jais P. Detailed analysis of the relation between bipolar electrode spacing and far- and near-field electrograms. *JACC Clin Electrophysiol*. 2019;5:66–77. doi:10.1016/j.jacep.2018.08.022
8. Tung R, Josephson ME, Bradfield JS, Shivkumar K. Directional influences of ventricular activation on myocardial scar characterization: voltage mapping with multiple wavefronts during ventricular tachycardia ablation. *Circ Arrhythm Electrophysiol*. 2016;9:e004155. doi:10.1161/CIRCEP.116.004155
9. Takigawa M, Relan J, Martin R, Kim S, Kitamura T, Frontera A, Cheniti G, Vlachos K, Massoulié G, Martin CA, Thompson N, Wolf M, Bourier F, Lam A, Duchateau J, Klotz N, Pambrun T, Denis A, Derval N, Magat J, Naulin J, Merle M, Collot F, Quesson B, Cochet H, Hocini M, Haïssaguerre M, Sacher F, Jais P. Importance of bipolar electrode orientation on local electrogram properties. *Heart Rhythm*. 2018;17:S1547–5271(18)30697-0. doi: 10.1016/j.hrthm.2018.07.020
10. Brunckhorst CB, Delacretaz E, Soejima K, Jackman WM, Nakagawa H, Kuck KH, Ben-Haim SA, Seifert B, Stevenson WG. Ventricular mapping during atrial and right ventricular pacing: relation of electrogram parameters to ventricular tachycardia reentry circuits after myocardial infarction. *J Interv Card Electrophysiol*. 2004;11:183–191. doi: 10.1023/B:JICE.0000048568.83404.59
11. Cochet H, Komatsu Y, Sacher F, Jadidi AS, Scherr D, Riffaud M, Derval N, Shah A, Roten L, Pascale P, Relan J, Sermesant M, Ayache N, Montaudon M, Laurent F, Hocini M, Haïssaguerre M, Jais P. Integration of merged delayed-enhanced magnetic resonance imaging and multide-tector computed tomography for the guidance of ventricular tachycardia ablation: a pilot study. *J Cardiovasc Electrophysiol*. 2013;24:419–426. doi: 10.1111/jce.12052
12. Amado LC, Gerber BL, Gupta SN, Rettmann DW, Szarf G, Schock R, Nasir K, Kraitzman DL, Lima JA. Accurate and objective infarct sizing by contrast-enhanced magnetic resonance imaging in a canine myocardial infarction model. *J Am Coll Cardiol*. 2004;44:2383–2389. doi: 10.1016/j.jacc.2004.09.020
13. Olimulder MA, Kraaier K, Galjee MA, Scholten MF, van Es J, Wagenaar LJ, van der Palen J, von Birgelen C. Infarct tissue characterization in implantable cardioverter-defibrillator recipients for primary versus secondary prevention following myocardial infarction: a study with contrast-enhancement cardiovascular magnetic resonance imaging. *Int J Cardiovasc Imaging*. 2013;29:169–176. doi: 10.1007/s10554-012-0077-6
14. Roes SD, Borleffs CJ, van der Geest RJ, Westenberg JJ, Marsan NA, Kaandorp TA, Reiber JH, Zeppenfeld K, Lamb HJ, de Roos A, Schalij MJ, Bax JJ. Infarct tissue heterogeneity assessed with contrast-enhanced MRI predicts spontaneous ventricular arrhythmia in patients with ischemic cardiomyopathy and implantable cardioverter-defibrillator. *Circ Cardiovasc Imaging*. 2009;2:183–190. doi: 10.1161/CIRCIMAGING.108.826529
15. West JJ, Patel AR, Kramer CM, Helms AS, Olson ES, Rangavajhala V, Ferguson JD. Dynamic registration of preablation imaging with a catheter geometry to guide ablation in a swine model: validation of image integration and assessment of catheter navigation accuracy. *J Cardiovasc Electrophysiol*. 2010;21:81–87. doi: 10.1111/j.1540-8167.2009.01572.x
16. Takigawa M, Martin R, Cheniti G, Kitamura T, Vlachos K, Frontera A, Martin CA, Bourier F, Lam A, Pillois X, Duchateau J, Klotz N, Pambrun T, Denis A, Derval N, Hocini M, Haïssaguerre M, Sacher F, Jais P, Cochet H. Detailed comparison between the wall thickness and voltages in chronic myocardial infarction. *J Cardiovasc Electrophysiol*. 2019;30:195–204. doi: 10.1111/jce.13767
17. Tung R, Kim S, Yagishita D, Vaseghi M, Ennis DB, Ouadah S, Ajjola OA, Bradfield JS, Mahapatra S, Finn P, Shivkumar K. Scar voltage threshold determination using ex vivo magnetic resonance imaging integration in a porcine infarct model: Influence of interelectrode distances and three-dimensional spatial effects of scar. *Heart Rhythm*. 2016;13:1993–2002. doi: 10.1016/j.hrthm.2016.07.003
18. Berrueto A, Fernández-Armenta J, Andreu D, Penela D, Herczku C, Evertz R, Cipolletta L, Acosta J, Borràs R, Arbelo E, Tolosana JM, Brugada J, Mont L. Scar dechanneling: new method for scar-related left ventricular tachycardia substrate ablation. *Circ Arrhythm Electrophysiol*. 2015;8:326–336. doi: 10.1161/CIRCEP.114.002386
19. Silberbauer J, Oloriz T, Maccabelli G, Tsiachris D, Baratto F, Vergara P, Mizuno H, Bisceglia C, Marzi A, Sora N, Guarracini F, Radinovic A, Cireddu M, Sala S, Gulletta S, Paglino G, Mazzone P, Trevisi N, Della Bella P. Non-inducibility and late potential abolition: a novel combined prognostic procedural end point for catheter ablation of postinfarction ventricular tachycardia. *Circ Arrhythm Electrophysiol*. 2014;7:424–435. doi: 10.1161/CIRCEP.113.001239
20. Di Biase L, Burkhardt JD, Lakkireddy D, Carbucicchio C, Mohanty S, Mohanty P, Trivedi C, Santangeli P, Bai R, Forleo G, Horton R, Bailey S, Sanchez J, Al-Ahmad A, Hranitzky P, Gallinghouse GJ, Pelargonio G, Hongo RH, Beheiry S, Hao SC, Reddy M, Rossillo A, Themistoclakis S, Dello Russo A, Casella M, Tondo C, Natale A. Ablation of stable VTs versus substrate ablation in ischemic cardiomyopathy: the VISTA randomized multicenter trial. *J Am Coll Cardiol*. 2015;66:2872–2882. doi: 10.1016/j.jacc.2015.10.026
21. Tzou WS, Frankel DS, Hegeman T, Supple GE, Garcia FC, Santangeli P, Katz DF, Sauer WH, Marchlinski FE. Core isolation of critical arrhythmia elements for treatment of multiple scar-based ventricular tachycardias. *Circ Arrhythm Electrophysiol*. 2015;8:353–361. doi: 10.1161/CIRCEP.114.002310
22. Jais P, Maury P, Khairy P, Sacher F, Nault I, Komatsu Y, Hocini M, Forclaz A, Jadidi AS, Weerasooriya R, Shah A, Derval N, Cochet H, Knecht S, Miyazaki S, Linton N, Rivard L, Wright M, Wilton SB, Scherr D, Pascale P, Roten L, Pederson M, Bordachar P, Laurent F, Kim SJ, Ritter P, Clementy J, Haïssaguerre M. Elimination of local abnormal ventricular activities: a new end point for substrate modification in patients with scar-related ventricular tachycardia. *Circulation*. 2012;125:2184–2196. doi: 10.1161/CIRCULATIONAHA.111.043216
23. Kienzle MG, Miller J, Falcone RA, Harken A, Josephson ME. Intraoperative endocardial mapping during sinus rhythm: relationship to site of origin of ventricular tachycardia. *Circulation*. 1984;70:957–965. doi: 10.1161/01.cir.70.6.957
24. Magtibay K, Massé S, Asta J, Kusha M, Lai PFH, Azam MA, Porta-Sanchez A, Haldar S, Malebranche D, Labos C, Deno DC, Nanthakumar K. Physiological assessment of ventricular myocardial voltage using omnipolar electrograms. *J Am Heart Assoc*. 2017;16:e006447. doi:10.1161/JAHA.117.006447